Model-Based Strategies for Biomedical Image Analysis: LV Strain Analysis from 4DE

James S. Duncan

Image Processing and Analysis Group

Departments of Biomedical Engineering, Diagnostic Radiology and Electrical Engineering

Yale University

College de France
June 24, 2014

Outline

I. Introduction

- Recovering Quantitative Information From Biomedical Images: an ill-posed problem
- Models as a substrate for recovery
- Underlying example in this talk: recovery of cardiac strain from echocardiography
- Current computational idea running through our work: sparse representations

II. Geometrical Models for Segmenting Structure

- deformable boundary models
- sparse coding/dictionary learning of appearance for boundary finding

III. Physical Models for Recovery of Soft Tissue Deformation

- measurement of left ventricular (cardiac) strain from 4D images
- sparse coding/dictionary learning for finding dense displacement vector fields

IV. Conclusions/Remaining Challenges

Image Analysis Systems Incorporate Quantitative Models and Use Mathematical Decision Making

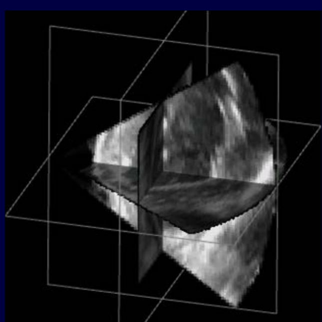

3D/4D Image

Feature detector

Model

Mathematical decision maker

Image-derived quantitative information

What types of models are useful for quantitative image analysis ?

- Size/shape/appearance of anatomical structure
- Size/shape of abnormal structure (e.g. tumors)
- Coherent functional information (e.g. time series)
- Motion/Deformation characteristics/ physiological information

Where do useful models come from ?

- Typically geometry, functional relations or physics
- in biomedical world: guided by anatomy, physiology (or biology)

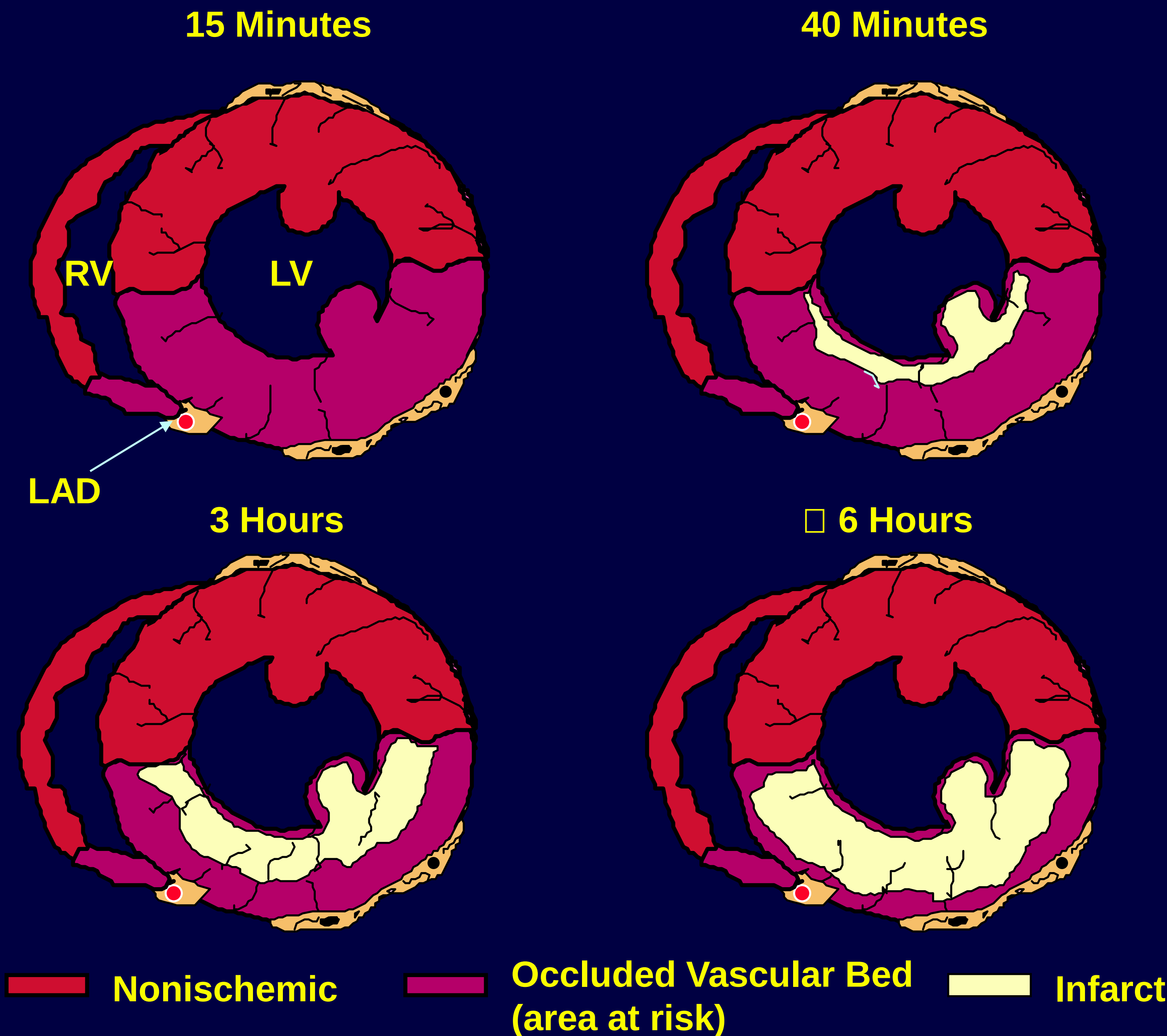
15 Minutes
40 Minutes
RV
LV
LAD
3 Hours
□ 6 Hours
Nonischemic
Occluded Vascular Bed
(area at risk)
Infarct

Example 4DE Image Dataset

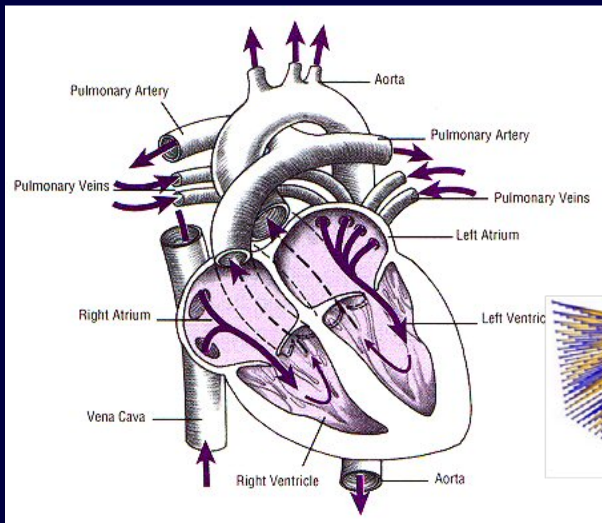

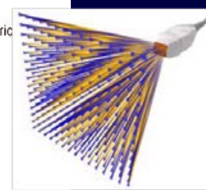

Philips iE33 system w/ X7-2 probe

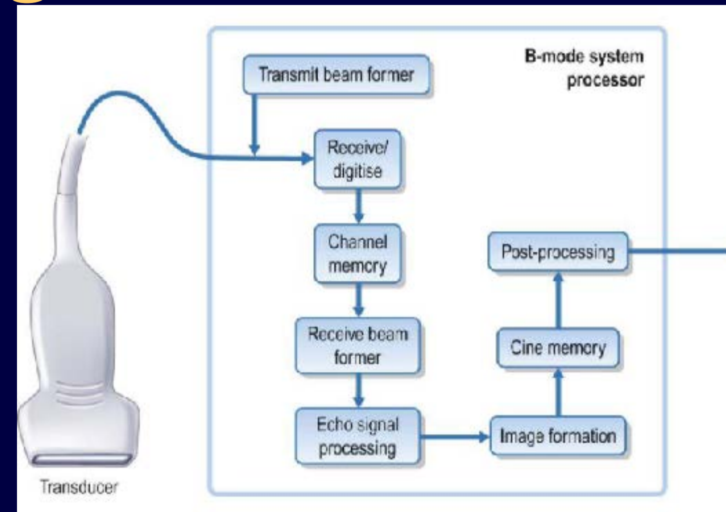

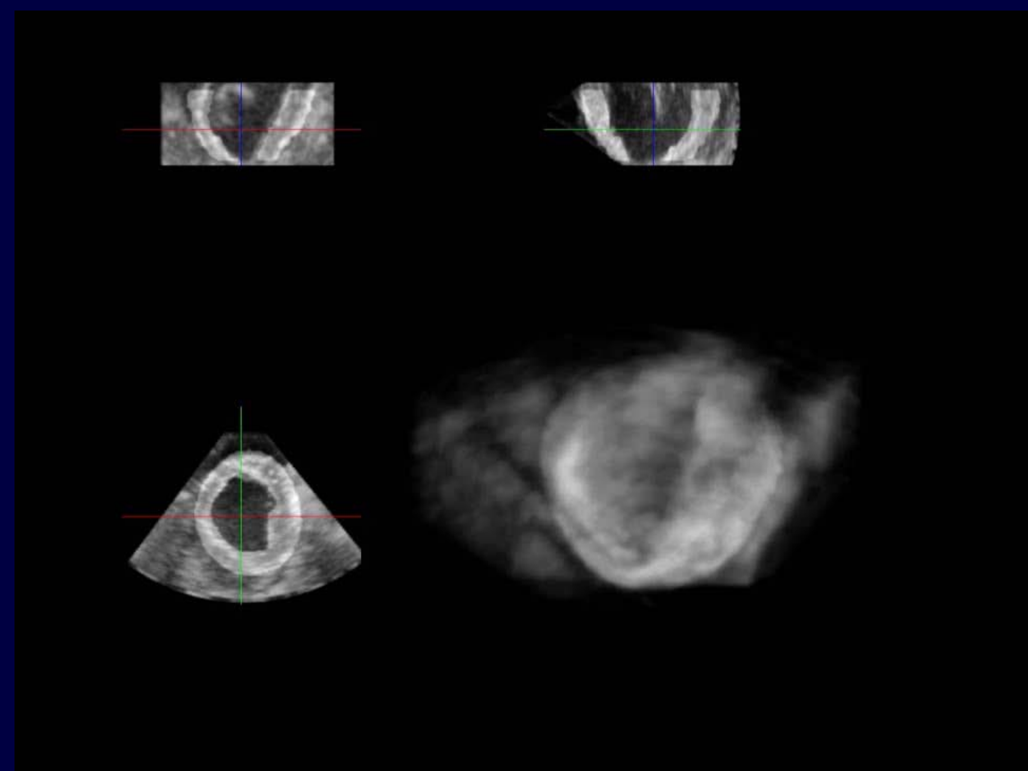

Center freq = 4.4 MHz
Aperture = 9.25mm x 9.25mm
Transmit focal depth = programmable
FOV = 90 degrees x 90 degrees

Volume frame rates = ~ 40Hz

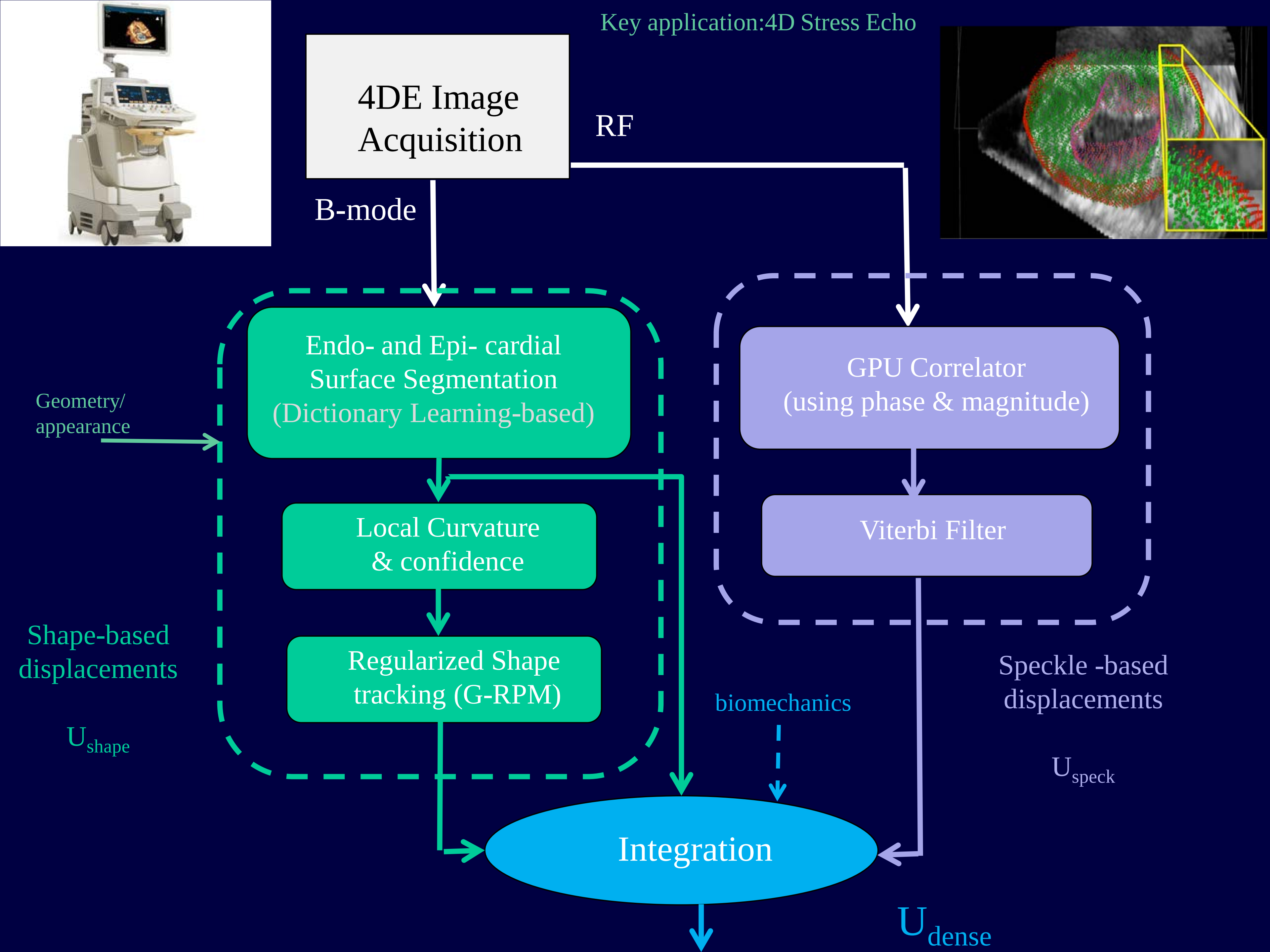
Key application:4D Stress Echo
4DE Image Acquisition
RF
B-mode
Endo- and Epi- cardial Surface Segmentation (Dictionary Learning-based)
Geometry/ appearance
Local Curvature & confidence
Regularized Shape tracking (G-RPM)
GPU Correlator (using phase & magnitude)
Viterbi Filter
Shape-based displacements
U_{shape}
Speckle -based displacements
U_{speck}
biomechanics
Integration
U_{dense}

II. Geometrical Models:

Object Segmentation

Multiframe Model for Cardiac Segmentation

- $I_{1:N} = \{I_1, I_2, \ldots I_N\}$ is a given cardiac sequence
- $\mathbf{s}_t$ is the segmentation at frame t
- Chan-Vese Level Sets – point sampled

$$\hat{\mathbf{s}}_t = \arg\max_{\mathbf{s}_t} P(\mathbf{s}_t \mid I_{1:t}) = \arg\max_{\mathbf{s}_t} P(I_t \mid \mathbf{s}_t, I_{1:t-1}) P(\mathbf{s}_t \mid I_{1:t-1})$$

$$= \arg\max_{\mathbf{s}_t} \underbrace{P(I_t \mid \mathbf{s}_t)}_{\text{data adherence}} \underbrace{P(\mathbf{s}_t \mid \hat{\mathbf{s}}_{1:t-1})}_{\text{dynamical shape prior}}$$

Nakagami pdf model for 3DE, Gaussian for MRI

Data Adherence (Likelihood) Term

Use Nakagami distribution (Shankar 2000) : compromise between Rayleigh (fully-developed speckle), pre-Rayleigh (weak) and post-Rayleigh (periodically-distributed speckles)

- LV Blood Pool
- LV Myocardium
- Background

$$P_1(I) = \frac{2\mu_1^{\mu_1}}{\Gamma(\mu_1)\omega_1^{\mu_1}} I^{2\mu_1 - 1} \exp\left(-\frac{\mu_1}{\omega_1} I^2\right)$$

$$P_2(I) = \frac{2\mu_2^{\mu_2}}{\Gamma(\mu_2)\omega_2^{\mu_2}} I^{2\mu_2 - 1} \exp\left(-\frac{\mu_2}{\omega_2} I^2\right)$$

$$P_3(I) = \sum_{k=1}^{M} \alpha_k P_k\left(I; \mu_{3,k}, \omega_{3,k}\right)$$

$$\log P(I \mid \mathbf{s}) = \sum_{l=1}^{3} \int_{\Omega_l} \log P_l(I)\, d\mathbf{x}$$

Incorporating Multiframe/ Multisubject Information for Segmentation (Zhu, et al., MICCAI 2008)

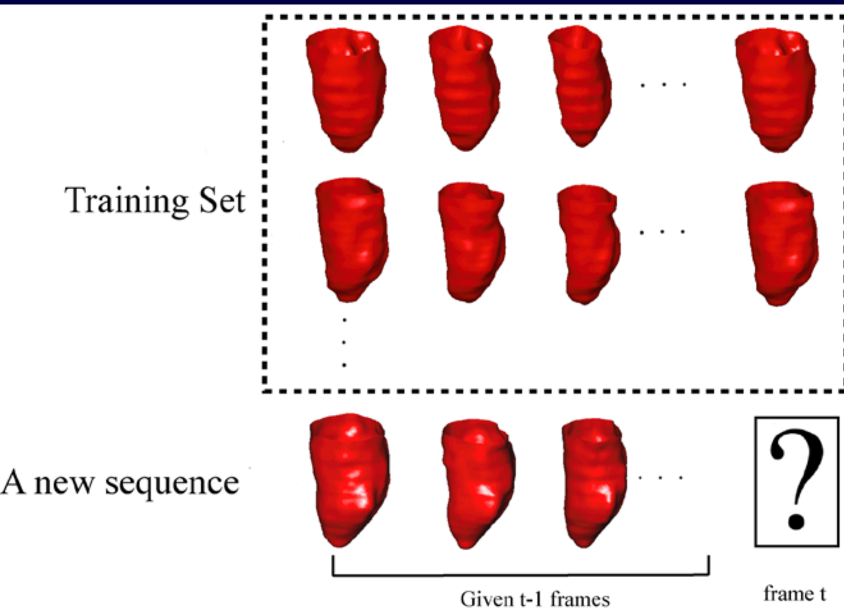

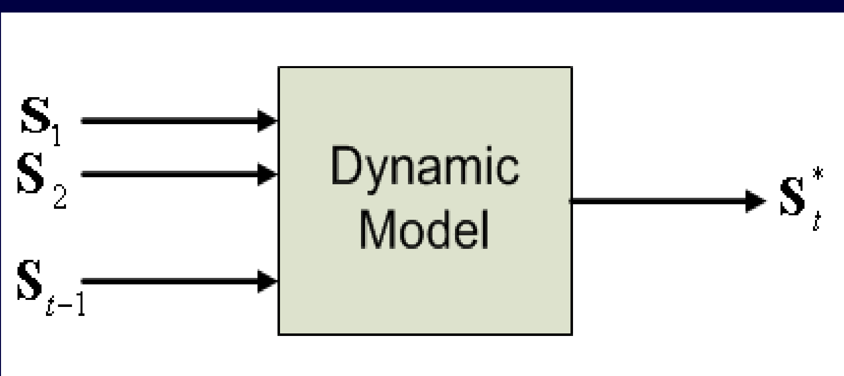

Training Phase (use tensor decomposition)

$$S = Z \times_1 \mathbf{V}^{\text{subject}} \times_2 \mathbf{V}^{\text{motion}} \times_3 \mathbf{V}^{\text{landmark}}$$

Prediction Phase

Step1 :projection

Segmentation of current sequence up to frame t-1

$$\hat{\mathbf{v}}^{\text{subject}} = B \times_1 \hat{\mathbf{S}}_{1:t-1}$$

$$B \ \alpha \ (Z^{-1} \times V^{\text{motion}^{-1}} \times V^{\text{landmark}^{-1}})$$

Step 2: prediction

$$\mathbf{S}_t^* = Z \times_1 \hat{\mathbf{v}}^{\text{subject}} \times_2 \mathbf{v}_t^{\text{motion}} \times_3 \mathbf{V}^{\text{landmark}}$$

Predicted segmentation at frame t based on frames 1:t-1 selecting info out of training space

Dynamical Shape Prior

$$P\left(\mathbf{S}_t \mid \hat{\mathbf{S}}_{1:t-1}\right) \propto \exp\left\{-\frac{\alpha}{2}\int \left\|\mathbf{S}_t - \mathbf{S}_t^*\right\|^2\right\}$$

Qualitative Results

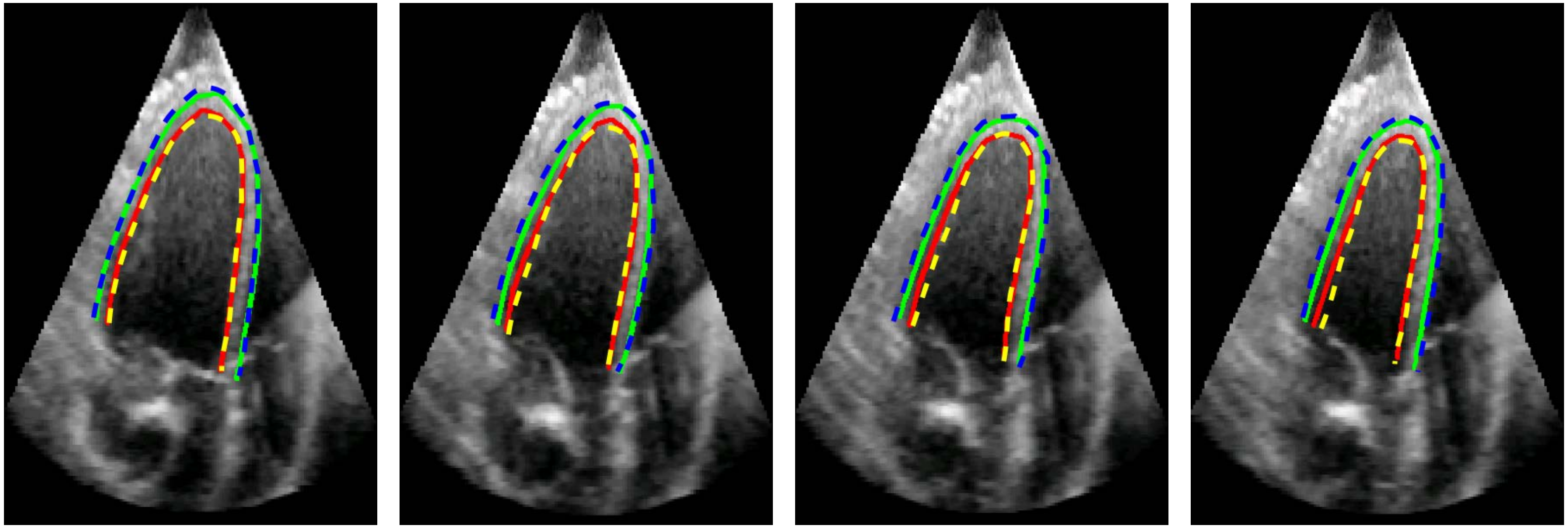

ED → ES

Solid Red: Automatic ENDO, Solid Green: Automatic EPI

Dotted Yellow: Manual ENDO, Dotted Blue: Manual EPI

3DRT typically w/ 20-22 frames over full cycle

Quantitative Evaluation
(3 Algorithms compared vs. Manual Tracing)

N=15 open chest canine studies

RT3D images (20-22 frames) acquired w/ Philips iE33 system

A = auto (algorithm) segmentation B = manual segmentation ("gold standard")

Mean absolute distance (MAD)

$$\mathrm{MAD}(A,B)=\frac{1}{2}\left\{\frac{1}{N}\sum_{i=1}^{N}d\left(\mathbf{a}_i,B\right)+\frac{1}{M}\sum_{j=1}^{M}d\left(\mathbf{b}_j,A\right)\right\}$$

Hausdorff distance (HD)

$$\mathrm{HD}(A,B)=\frac{1}{2}\left\{\max_i d\left(\mathbf{a}_i,B\right)+\max_j d\left(\mathbf{b}_j,A\right)\right\}$$

Percentage of true positives

$$\mathrm{PTP}=\frac{\mathrm{Volume}\left(\Omega_A\cap\Omega_B\right)}{\mathrm{Volume}\left(\Omega_A\right)}$$

Quantitative Evaluation (cont.)

3 Algorithms tested vs. Manual Tracing:

- SSDM = Subject Specific Dynamic Model (Our approach)
- GDM = General Dynamic Model (prediction from previous 2 frames)
- SM = Static Model (PDM-like)

Mean absolute distance (MAD)

Hausdorff distance (HD)

Percentage of true positives

		MAD (mm)	HD (mm)	PTP (%)
ENDO	automatic-manual (SSDM)	1.41 ± 0.40	2.53 ± 0.75	95.9 ± 1.24
	automatic-manual (GDM)	1.52 ± 0.46	3.25 ± 0.98	94.8 ± 1.56
	automatic-manual (SM)	2.33 ± 0.67	4.31 ± 1.26	93.1 ± 1.51
EPI	automatic-manual (SSDM)	1.74 ± 0.39	2.79 ± 0.97	94.5 ± 1.74
	automatic-manual (GDM)	1.77 ± 0.41	2.91 ± 0.95	93.6 ± 1.78
	automatic-manual (SM)	1.81 ± 0.65	3.18 ± 1.23	92.3 ± 1.91

Mean and SD over all points X all frames X all subjects

Dynamical Appearance Model

- **A database-free contour tracking framework**
  - A dynamical appearance model
  - Individual data coherence; spatiotemporal constraint
  - Multiscale sparse representation; dictionary learning
  - First work applying sparse modeling to this problem
  - Level sets; maximum a posteriori (MAP) estimation
-

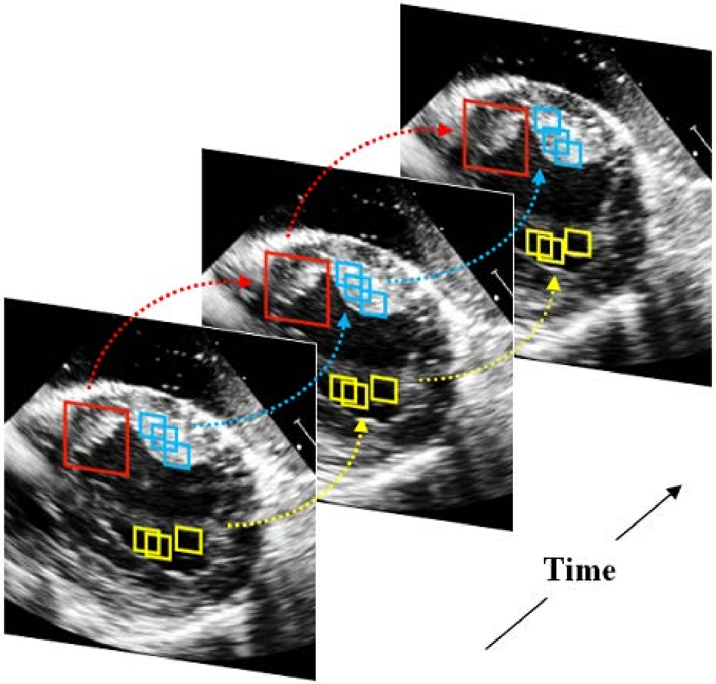

LV Segmentation via Online Dictionary Learning

(Huang, et al, MICCAI, 2012; Huang, et al., *Medical Image Analysis*, Nov, 2013)

Sparse Representation

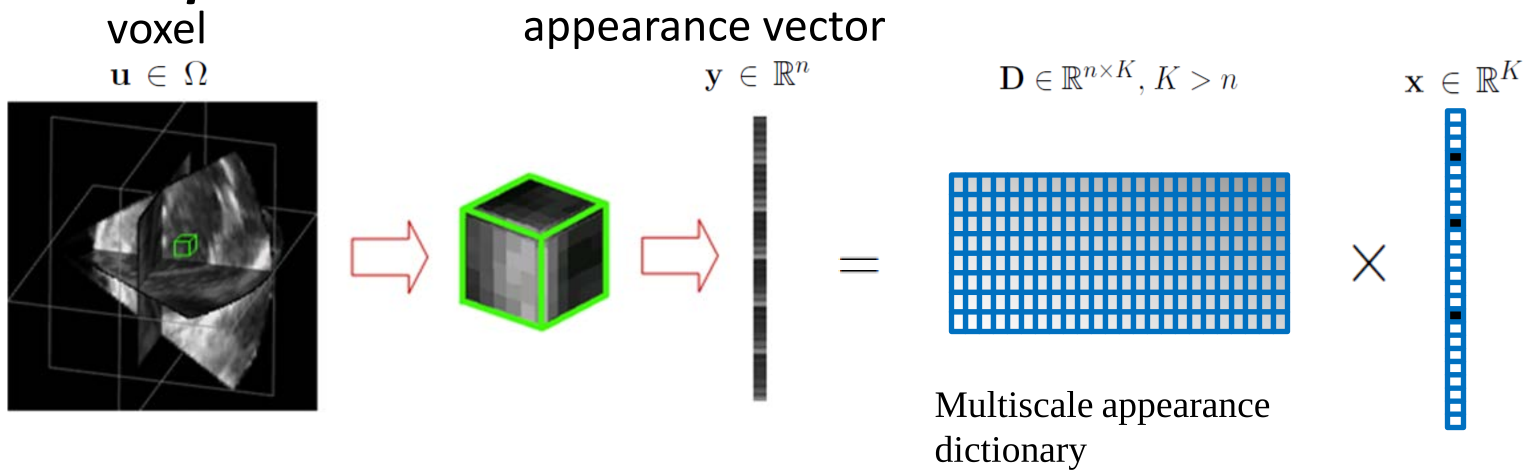

Online Dictionary Learning

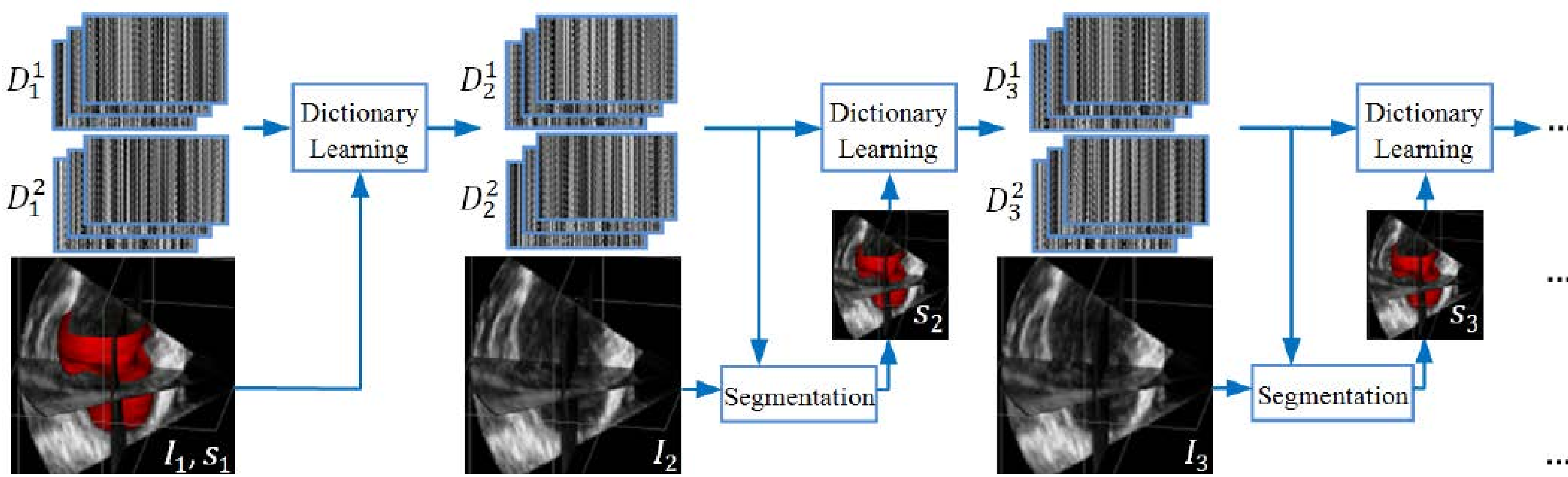

Dynamical dictionary update interlaced with sequential segmentation.

Pairs of dictionaries are learned at each scale using AdaBoost where multiple weak learners are found by varying one column at a time per scale…..and then multiple scales are combined.

Examples of learned dictionaries

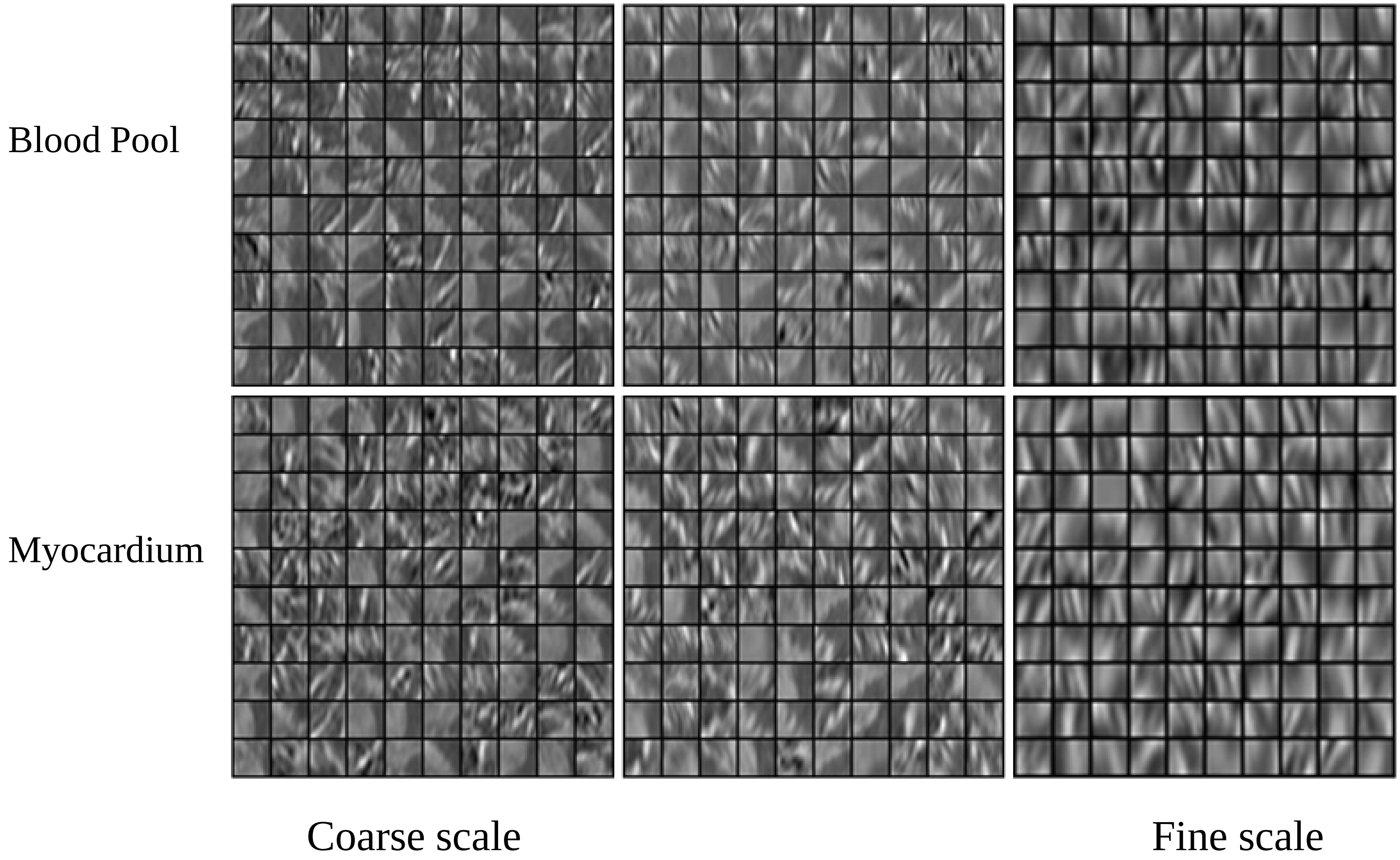

Two problems in sparse modeling

- Sparse coding

$$\min_{\mathbf{x}} ||\mathbf{y} - \mathbf{D}\mathbf{x}||_2^2 \text{ s.t. } ||\mathbf{x}||_0 \leq T_0$$

Greedy algorithms: matching pursuit (MP), orthogonal matching pursuit (OMP), etc.
Convex optimization: least angle regression (LARS), coordinate descent, iterative shrinkage-thresholding algorithm (ISTA), etc.

- Dictionary learning (uses sparse coding at each step of Adaboost framework via k-SVD)

$$\min_{\mathbf{D},\mathbf{X}} ||\mathbf{Y} - \mathbf{D}\mathbf{X}||_2^2 \text{ s.t. } \forall i, ||\mathbf{x}_i||_0 \leq T_0$$

K-SVD, method of optimal directions (MOD), online dictionary learning (ODL), etc.

Dynamical appearance model

Sparse representation of local appearance

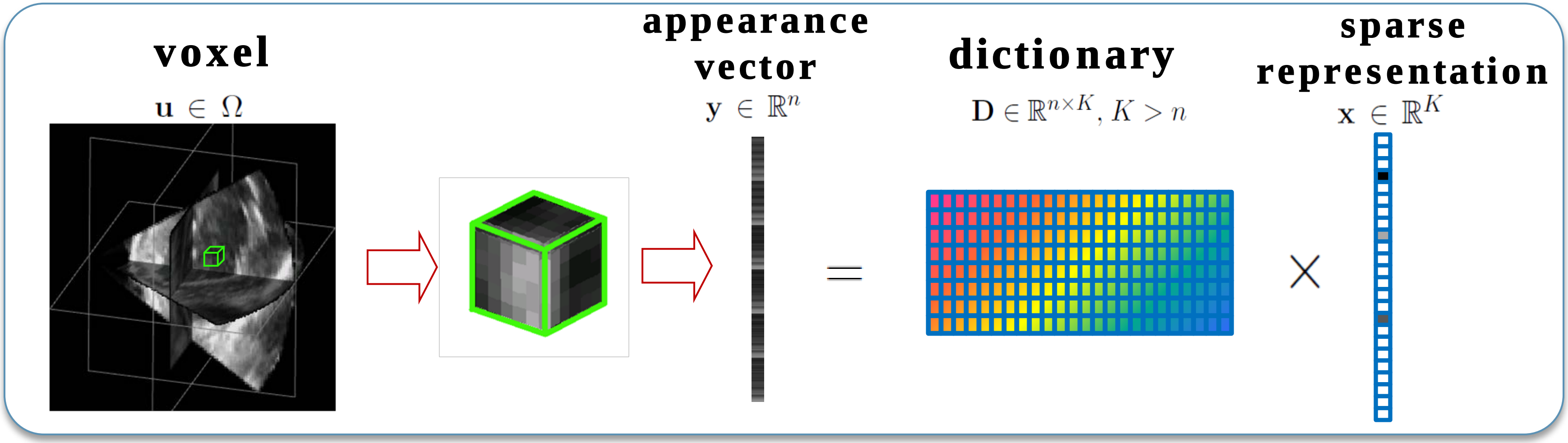

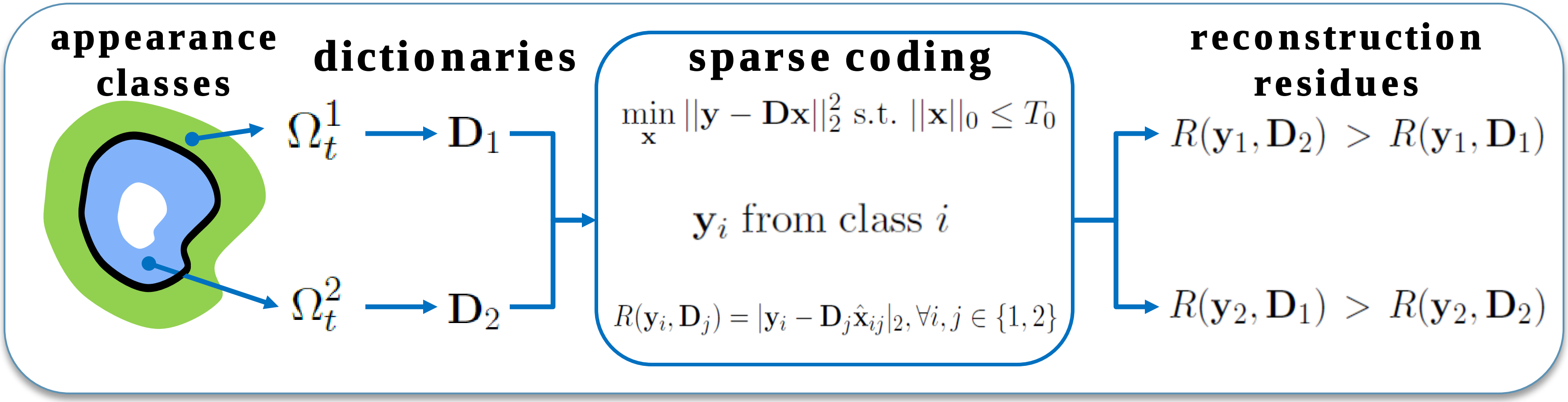

Residues computed in test data

LV Segmentation via Online Dictionary Learning

MAP Estimation

Goal: estimate the segmentation s_t of frame I_t, given $I_{1:t-1}$ and $s_{1:t-1}$.

$$
\begin{aligned}
\hat{\Phi}_t &= \arg\max\nolimits_{\Phi_t} p(\hat{\Phi}_{1:t-1}, I_{1:t-1}, I_t | \Phi_t) p(\Phi_t) \\
&\approx \arg\max\nolimits_{\Phi_t} p(\Phi_t^*, R_t, I_t | \Phi_t) p(\Phi_t) \\
&\approx \arg\max\nolimits_{\Phi_t} p(\Phi_t^* | \Phi_t) p(R_t | \Phi_t) p(I_t | \Phi_t) p(\Phi_t).
\end{aligned}
$$

Dynamical Shape Prediction

Local Appearance Discriminant (classes= myocard/outside)

Intensity

Experimental Results

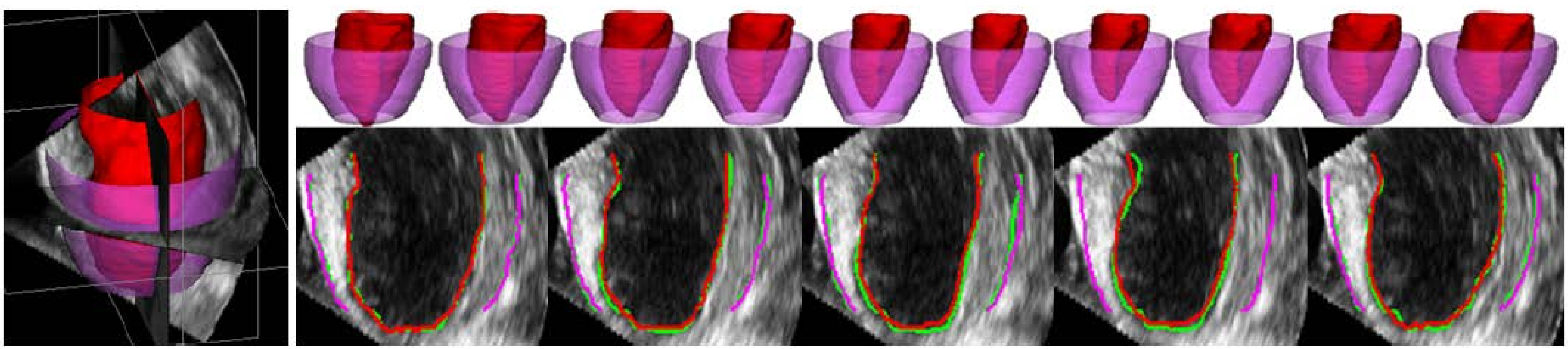

Typical segmentations by our method (red,purple) and manual tracings (green).

LV Segmentation via Online Dictionary Learning

Experimental Results (Contd.)

expressed as mean±std		DICE (%)	PTP (%)	MAD (mm)	HD (mm)
Endocardial	Rayleigh [12]	74.9 ± 18.8	83.1 ± 16.3	2.01 ± 1.22	9.17 ± 3.37
	DAM	93.6 ± 2.49	94.9 ± 2.34	0.57 ± 0.14	2.95 ± 0.62
	SSDM [5]	——	95.9 ± 1.24	1.41 ± 0.40	2.53 ± 0.75
Epicardial	Rayleigh [12]	74.1 ± 17.4	82.5 ± 12.0	2.80 ± 1.55	16.9 ± 9.30
	DAM	97.1 ± 0.93	97.6 ± 0.86	0.60 ± 0.19	3.03 ± 0.76
	SSDM [5]	——	94.5 ± 1.74	1.74 ± 0.39	2.79 ± 0.97

DAM is just as good as SSDM w/o prior database

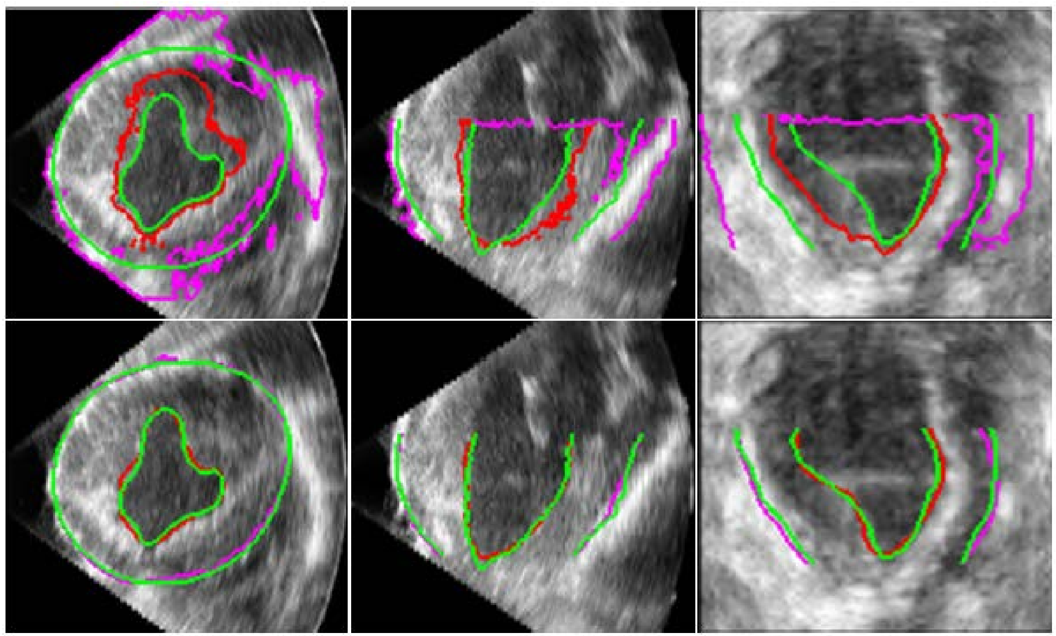

Figure 7. Comparisons of segmentation results by the Rayleigh model (top) and our DAM (bottom). Green: Manual. Red: Automatic endocardial. Purple: Automatic epicardial.

III. Physical Models:

Cardiac Motion/Deformation Analysis

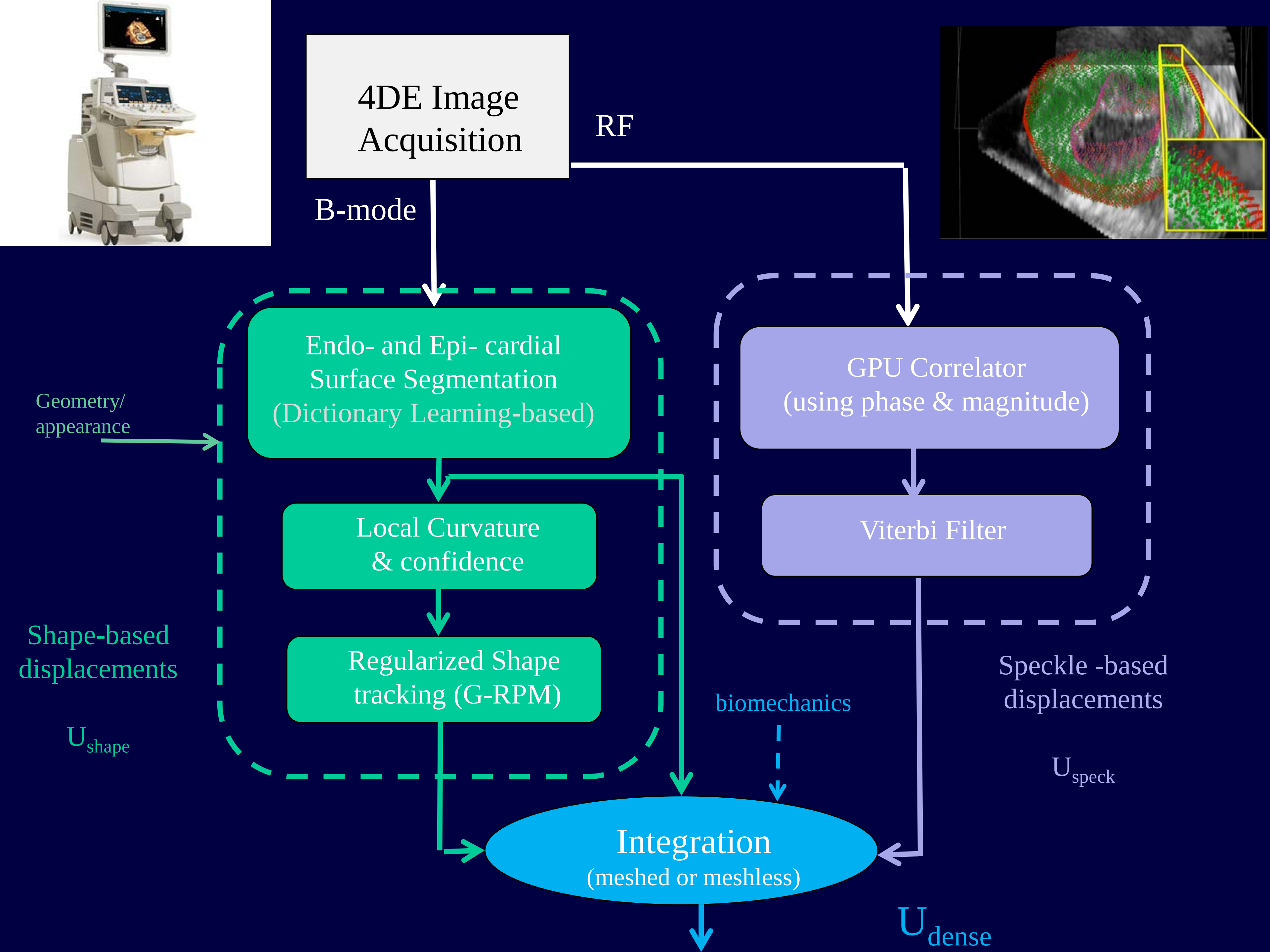
4DE Image Acquisition
RF
B-mode
Endo- and Epi- cardial Surface Segmentation (Dictionary Learning-based)
Geometry/ appearance
Local Curvature & confidence
Regularized Shape tracking (G-RPM)
Shape-based displacements
U_{shape}
GPU Correlator (using phase & magnitude)
Viterbi Filter
Speckle -based displacements
U_{speck}
biomechanics
Integration (meshed or meshless)
U_{dense}

Shape-Based Tracking of ED-ES Left Ventricular Displacements (Shi, Constable, Sinusas, Ritman,Duncan, IEEE TMI, 2000)

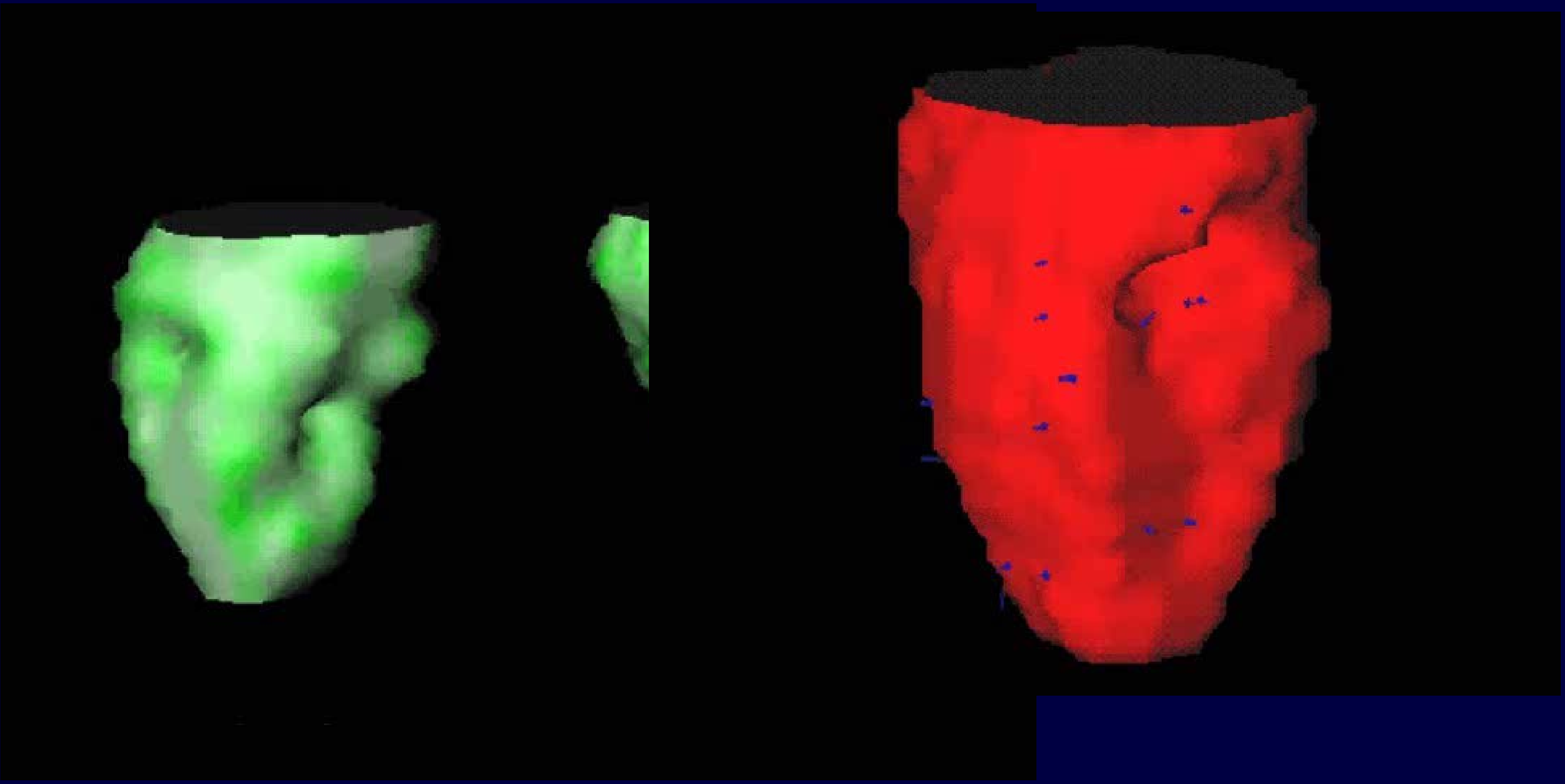

e.g., note Bending Energies:

$$\epsilon_{be}(u,v) = \kappa_1^2(u,v) + \kappa_2^2(u,v)$$

(White = less bending away from flat plane, Green= more bending)

RF-based Speckle Tracking from 4DE (M. O'Donnell, et al.)

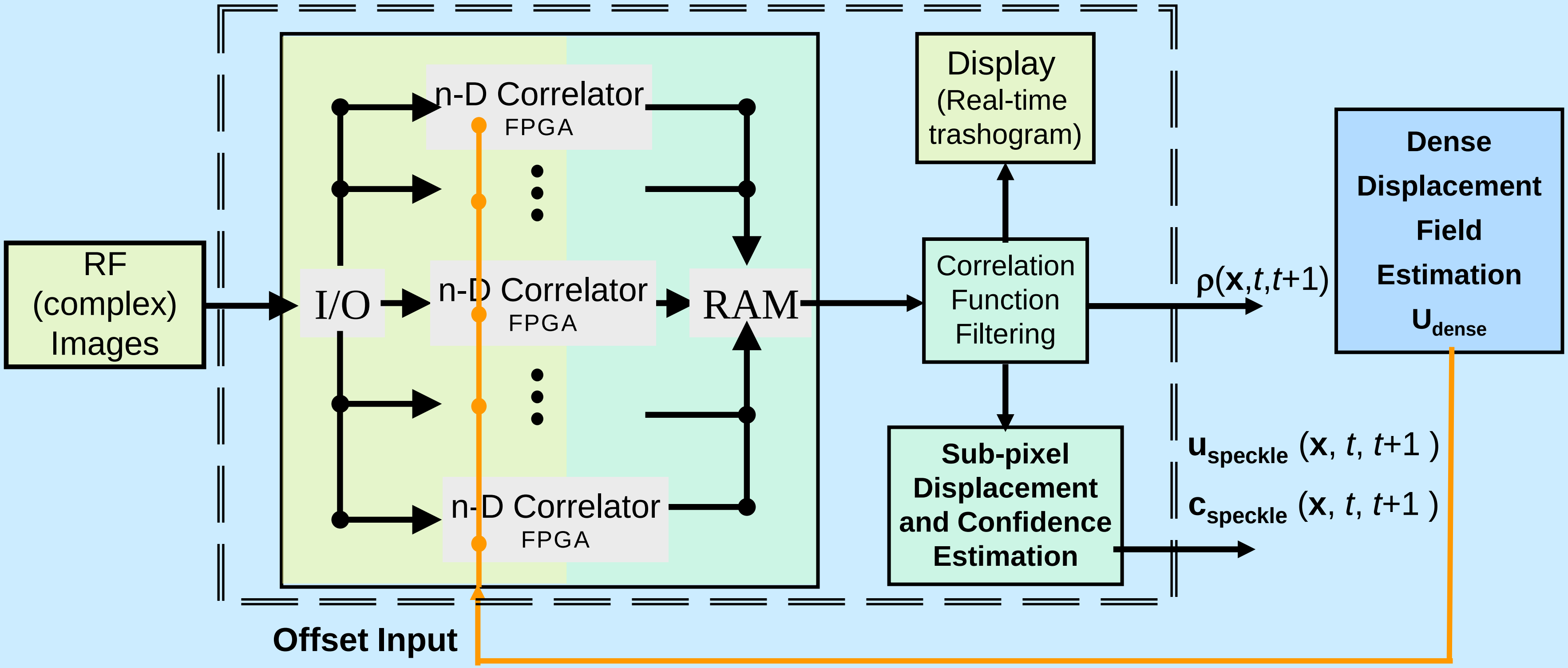

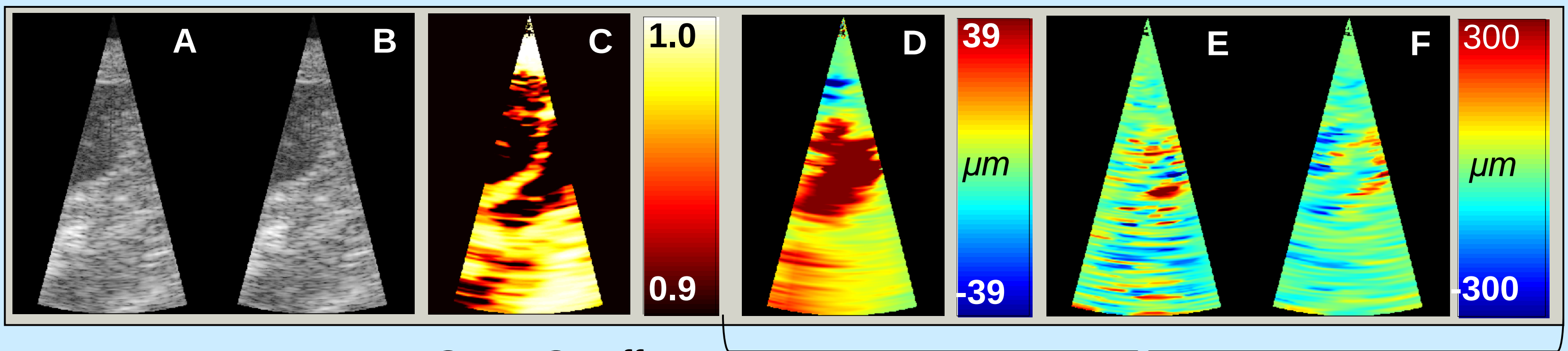

B-mode axial, elevation plane for t=16/ 40

Corr. Coeff t=16 to t=17 $\rho(\mathbf{x},t,t+1)$

Axial, elevational,lateral displacements t=16 to t=17 $\mathbf{u}_{speckle}(\mathbf{x}, t, t+1)$

Effect of Increasing Model Stiffness

$$C^{-1} = \begin{bmatrix} \frac{1}{E_p} & \frac{-\nu_{pp}}{E_p} & \frac{-\nu_{fp}}{E_f} & 0 & 0 & 0 \\ \frac{-\nu_{pp}}{E_p} & \frac{1}{E_p} & \frac{-\nu_{fp}}{E_f} & 0 & 0 & 0 \\ \frac{-\nu_{fp}E_f}{E_p} & \frac{-\nu_{fp}E_f}{E_p} & \frac{1}{E_f} & 0 & 0 & 0 \\ 0 & 0 & 0 & \frac{2(1+\nu_{pp})}{E_p} & 0 & 0 \\ 0 & 0 & 0 & 0 & \frac{1}{G_f} & 0 \\ 0 & 0 & 0 & 0 & 0 & \frac{1}{G_f} \end{bmatrix}$$

E_f = fiber stiffness
E_p = cross fiber stiffness ($E_f \sim 4E_p$)

ν_{fp}, ν_{pp} = corresponding Poisson's ratios (~.4)
$G_f \sim E_f / [2(1+ n_{fp})]$ (shear modulus across fibers)

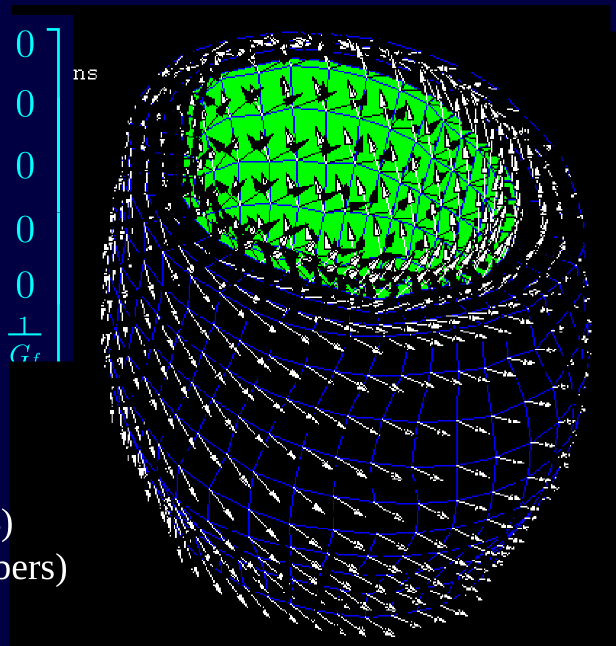

F_r = 5000 Pascal

F_c = 1000 Pascal

E = 20000 Pascal

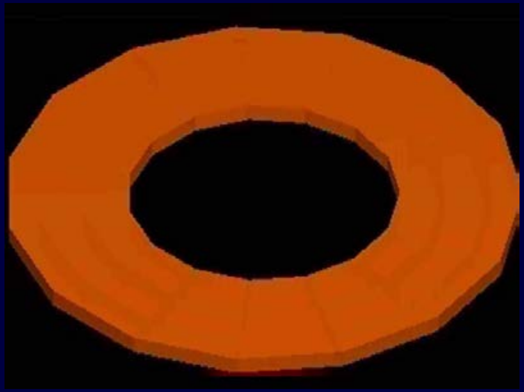

E = 40000

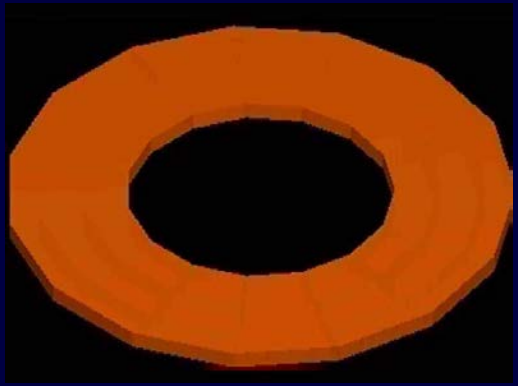

E = 70000

Solution via Finite Element Method

Now write the logarithmic version of the a-posteriori solution:

$$\hat{u} = \underset{u}{\arg\max} \left(\underbrace{\log p(u^m | u)}_{\text{Data Term}} + \underbrace{\log p(u)}_{\text{Model Term}} \right)$$

in vector/matrix form (with confidence $A = \Sigma^{-1}$):

$$\hat{U} = \max_U \; \Sigma_{\text{all elements}} \left[(U - U^m)^t A (U - U^m) + U^t K U \right]$$

Differentiating wrt U yields: $A(U - U^m) = KU$

which can be solved for U

Strain from MRI (Shape-Tracking: Sinusas, et al, AJP, 2003)

Normal Canine Heart

1 Hour Post- LAD Occlusion

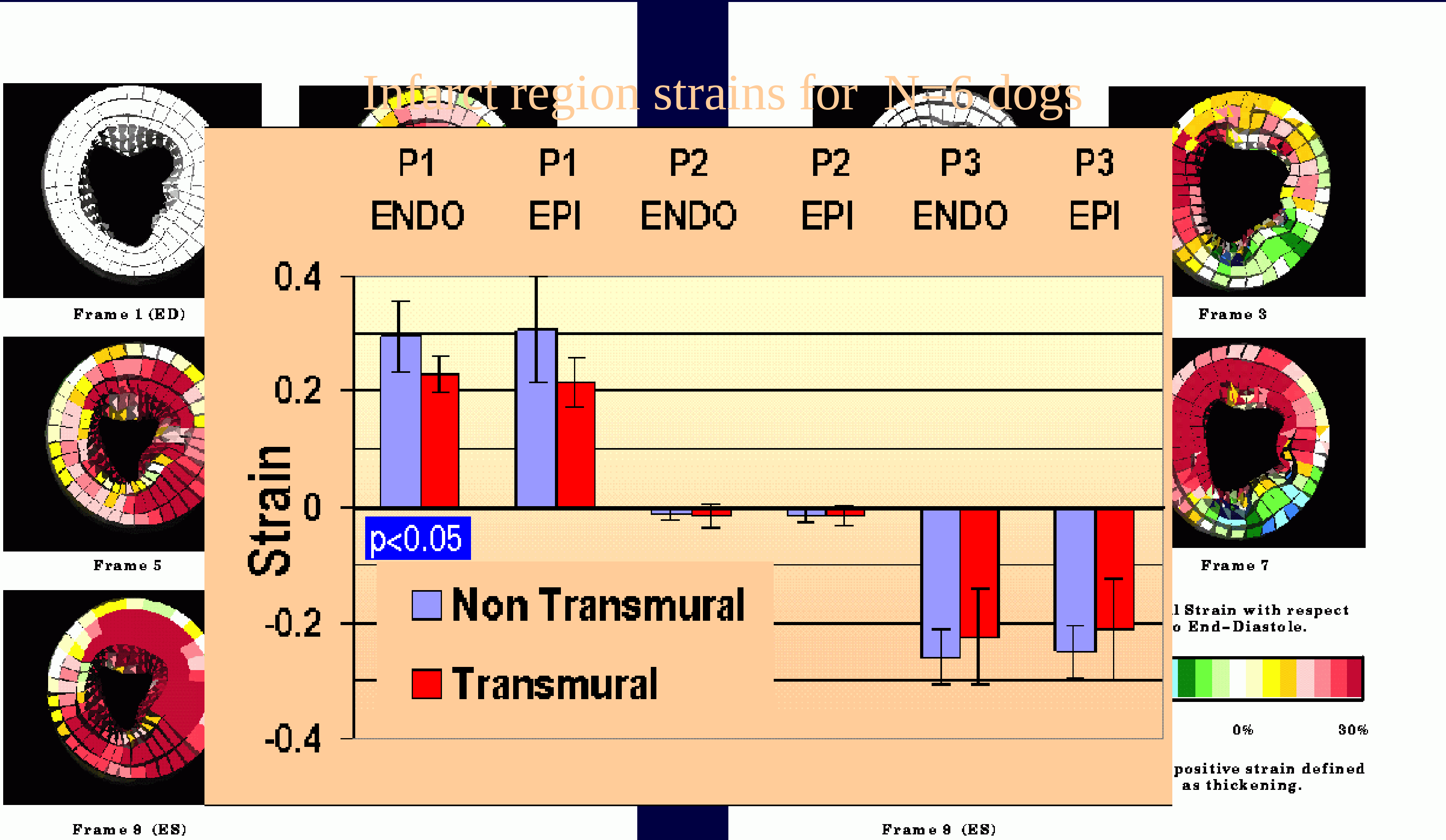

Sparse to Dense Displacements: Options

- <u>Free Form Deformation (FFD):</u>

  - must place control points on regular lattice
  - difficult to model complex geometries

- <u>Extended Free Form Deformation (EFFD):</u>

  - allows for complex geometry
  - complicated meshing procedure
  - segmentation necessary

- <u>Finite Element Method (FEM):</u>

  - sensitive to data distribution
  - computationally intensive
  - complicated formulation

- <u>Boundary Element Method (BEM):</u>

  - requires mapping of interior points to boundaries
  - difficult to implement for non-homogenous material

- **<u>Radial Basis Functions (RBF):</u>**

  - no meshing required
  - easy to model complex geometry
  - can either interpolate or approximate

Integration of Speckle (Green) and Shape (Red) Displacements (Compas, et al., *IEEE TMI*, Feb,2014)

- FEM Methods require meshing (difficult w/ certain geometries) & are computationally costly
- Recently moved toward combining the complementary shape and speckle-tracked information using mesh-free techniques: radial basis functions (RBFs)
- Model Deformation field as a linear combination of basis functions

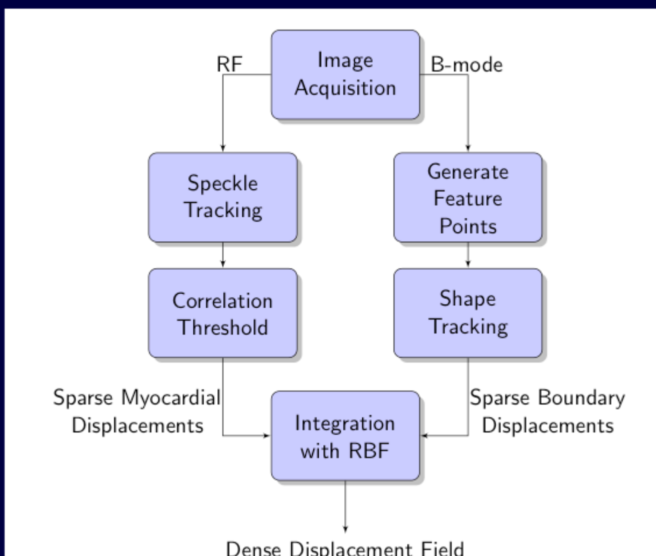

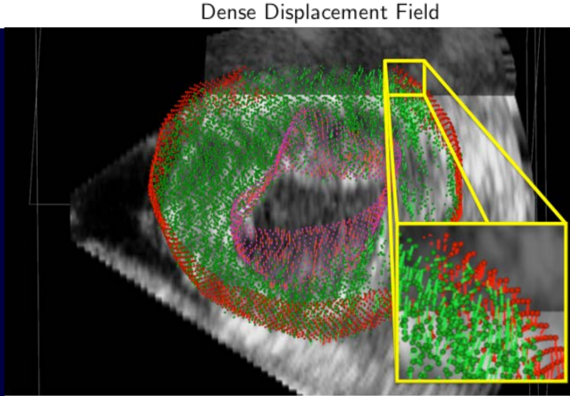

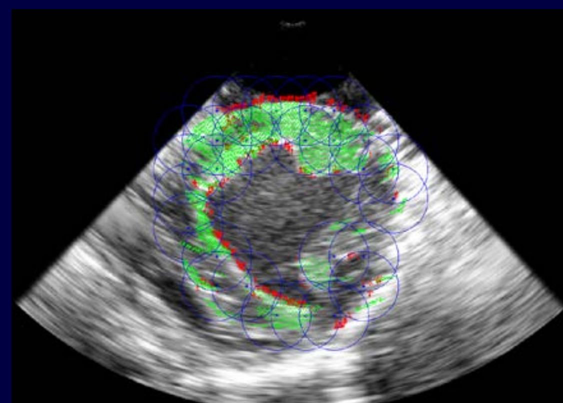

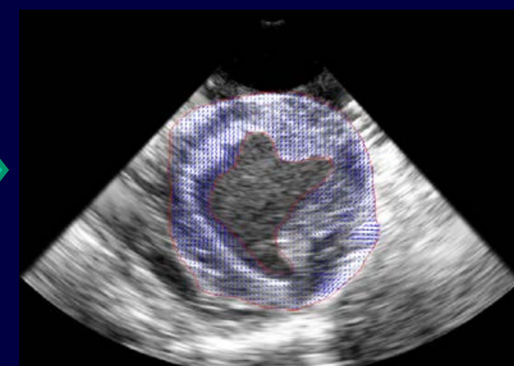

$$\hat{u} = \arg\max_{u} P(u/I_{rf}, I_{bm})$$

$$U(\mathbf{x}) = \sum_{k=1}^{N} \lambda_k \phi(||\mathbf{x} - \mathbf{x}_k||)$$

Sector-based Strain Comparison: Integrated 4DE vs MR tagging (N=8 dogs)

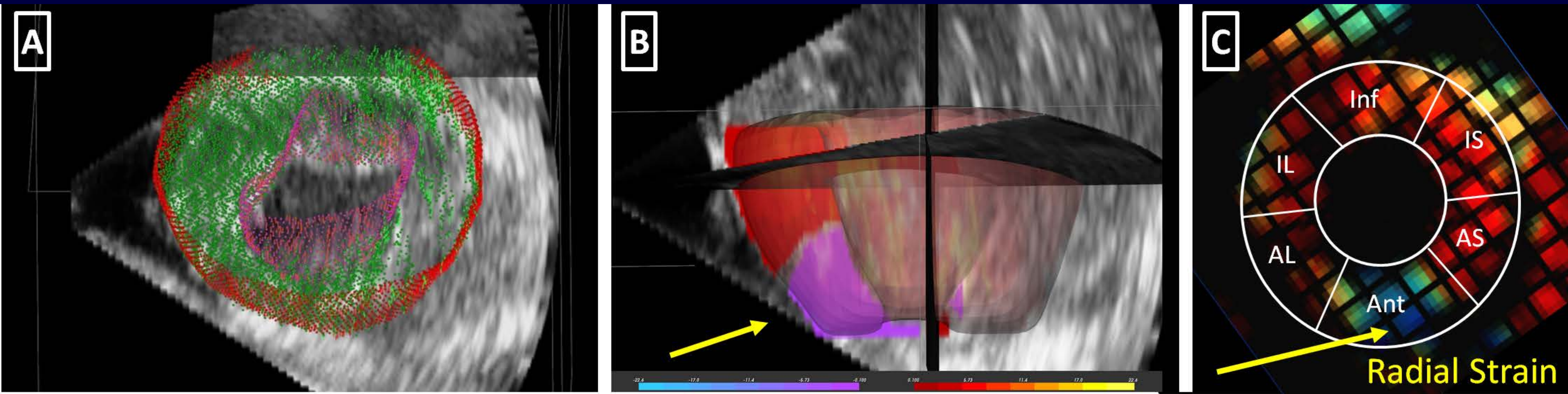

C	AS		IS		Inf		IL		AL		Ant	
	Radial	Circ.	Radial	Circ.	Radial	Circ.	Radial	Circ.	Radial	Circ.	Radial	Circ.
Apical	0.86	0.87	0.87	0.97	0.95	0.81	0.84	0.95	0.77	0.90	0.70	0.66
Medial Apical	0.92	0.93	0.93	0.97	0.88	0.79	0.85	0.86	0.67	0.89	0.81	0.95
Medial Basal	0.94	0.98	0.96	0.97	0.96	0.96	0.96	0.93	0.85	0.96	0.88	0.95
Basal	0.96	0.96	0.96	0.97	0.96	0.98	0.92	0.96	0.90	0.98	0.91	0.97

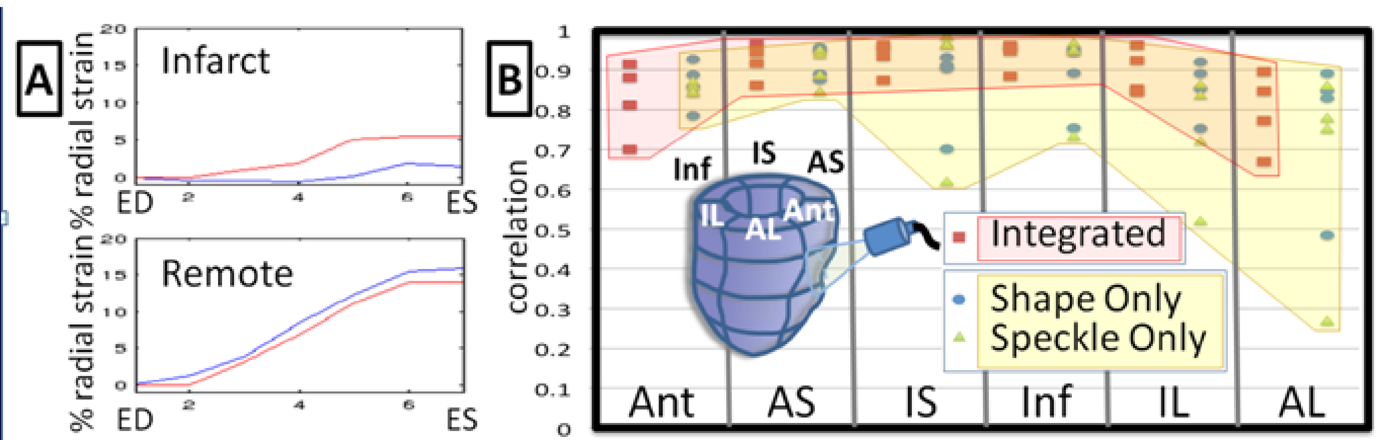

Radial Basis Function (RBF) interpolation Of Displacement Vector Fields: Sparsity Formulation

- Approximation of a function value at any point *x* is given by sum of values of N radial basis functions evaluated at any *x = < x, y, z >*:

$$f(\mathbf{x}) = \sum_{k=1}^{N} w_k \phi_{\sigma_k}(||\mathbf{x} - c_k||)$$

- Writing each radial basis function component as h_k, and consolidating them together as a matrix *H*, we can write the dense displacement estimates *U* as (in 2D):

$$U =< Hw_x, Hw_y >$$

- Solving for *U* is equivalent to solving for w_x and w_y.
- We can solve for w_x and w_y in the following way by using their l_1 norms as penalties:

$$\hat{w_x}, \hat{w_y} = \underset{w_x, w_y}{\operatorname{argmin}} \sum_{i \in A_{sh}} ||U(i) - U_{sh}(i)||_2^2 + \sum_{i \in A_{sp}} ||U(i) - U_{sp}(i)||_2^2 + \lambda ||w_x||_1 + \lambda ||w_y||_1$$

(A_{sh} and A_{sp} index the speckle tracked and shape tracked displacement values)

See also: S. Chen, D. Donoho, and M. Saunders. Atomic decomposition by basis pursuit. SIAM Review, 43(1):129–159, 2001.

RBFs as a dictionary and sparsity

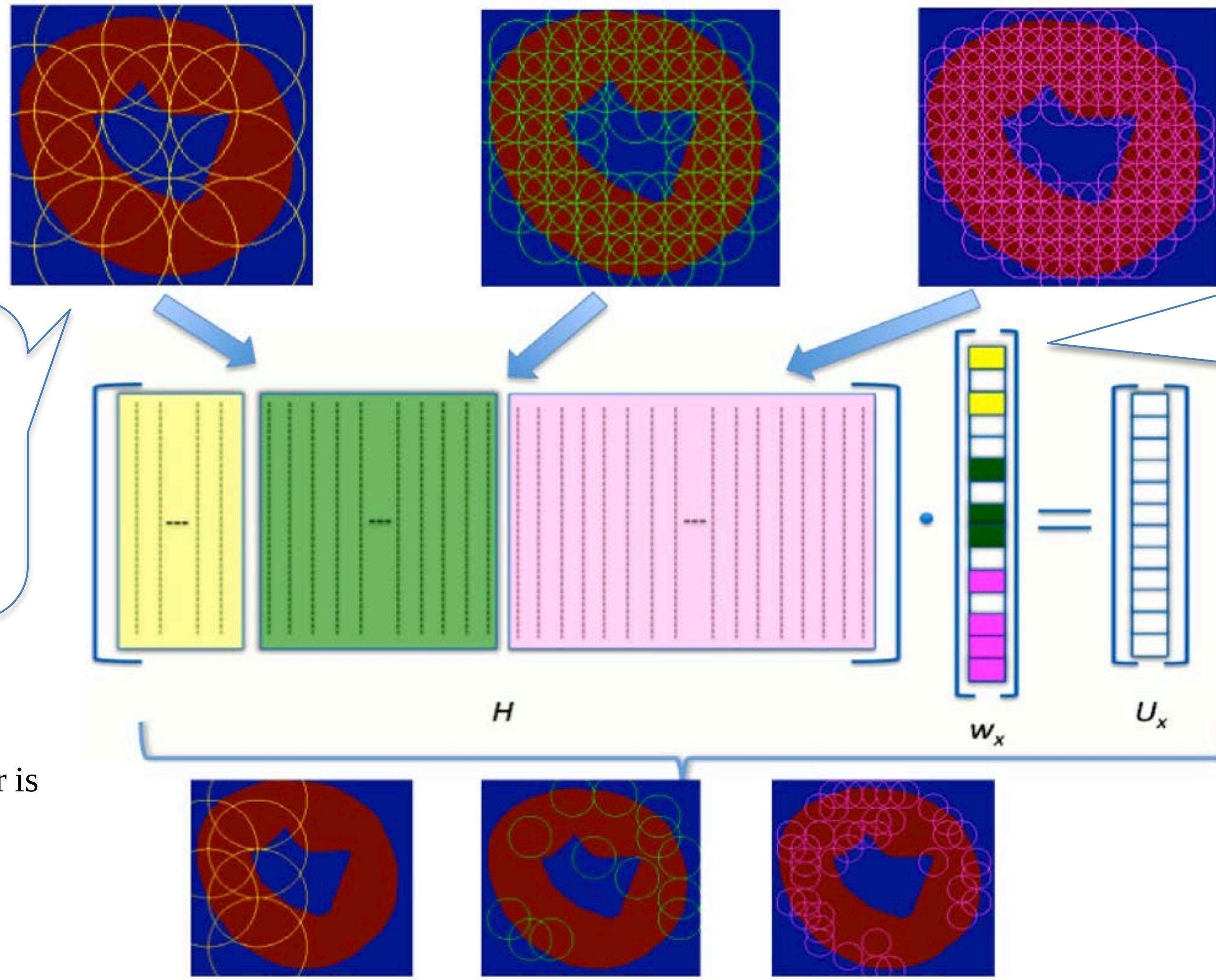

Radial basis functions of varying widths and positions.

Sparsity constraint forces several coefficients to be zero.

Each column vector is x,y(and z) position and a width

Fig: Figure displaying how radial basis functions of different widths and different positions are considered and implicitly chosen using the sparsity constraints. The yellow, green and pink colors encode the basis function variety.

Sparse coding with RBFs

- Because in practice minimizing l_1 norm leads to a sparse solution (Chen et al., 2001), in context of our problem, it means the weights corresponding to several basis functions will be zero.
- This implies that only certain number of basis functions we consider for interpolation are relevant.

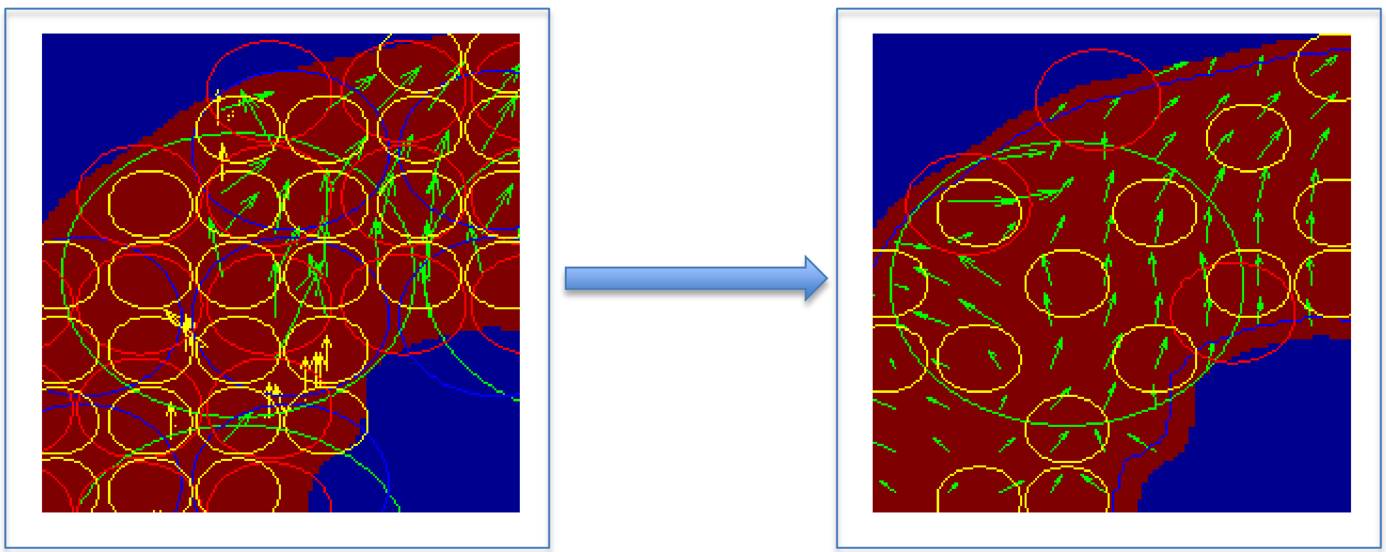

Fig: (left) Visualization of the RBF of different widths over sparse data. (Right) Only the significant RBFs, interpolating the dense field

Learning with RBFs

- The choice of the 'dictionary' of basis functions to carry out the interpolation is possibly an important determinant in the efficacy and the quality of the interpolation results.
- This is something we look to explore and hopefully exploit.
- Choosing a set of RBFs of different width profiles, would lead to a different dictionary. Based on the distribution of the data and the displacement values, we hope to learn the appropriate one.
- AT THE MOMENT: just find the sparsest coded combination of multiscale RBFs to fit data.....

- IN THE FUTURE: learn more efficient displacement dictionaries from collections of frames and/or training sets and apply to a test set (i.e. a multiframe, spatiotemporal displacement dictionary)

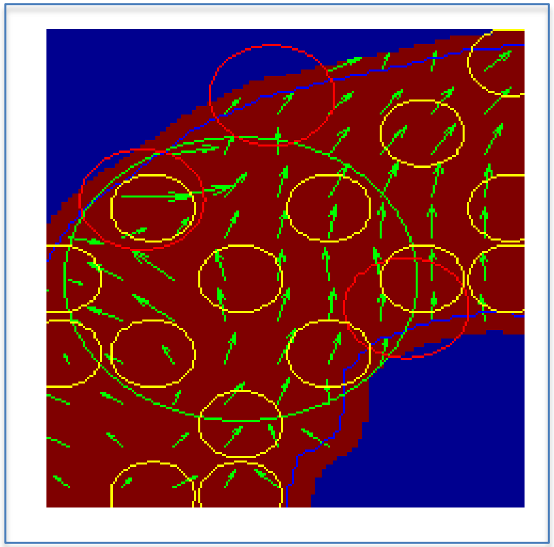

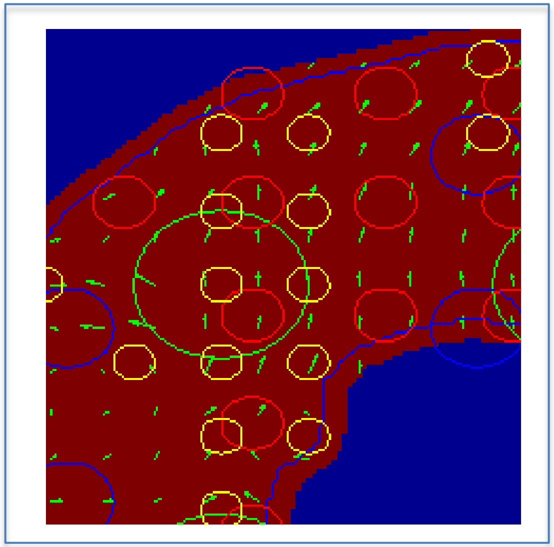

Fig: (left) Visualization of the RBF of different widths over dense data. (Right) RBFs of half the width on left used result in different orientations (scaling not exact)

Illustration (2D)

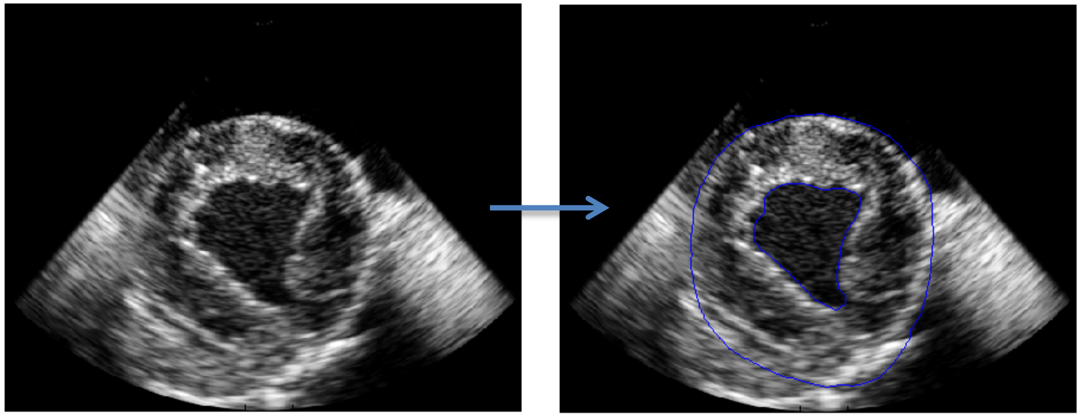

Fig: (left) B-mode image. (right) Region consisting of the myocardium displayed

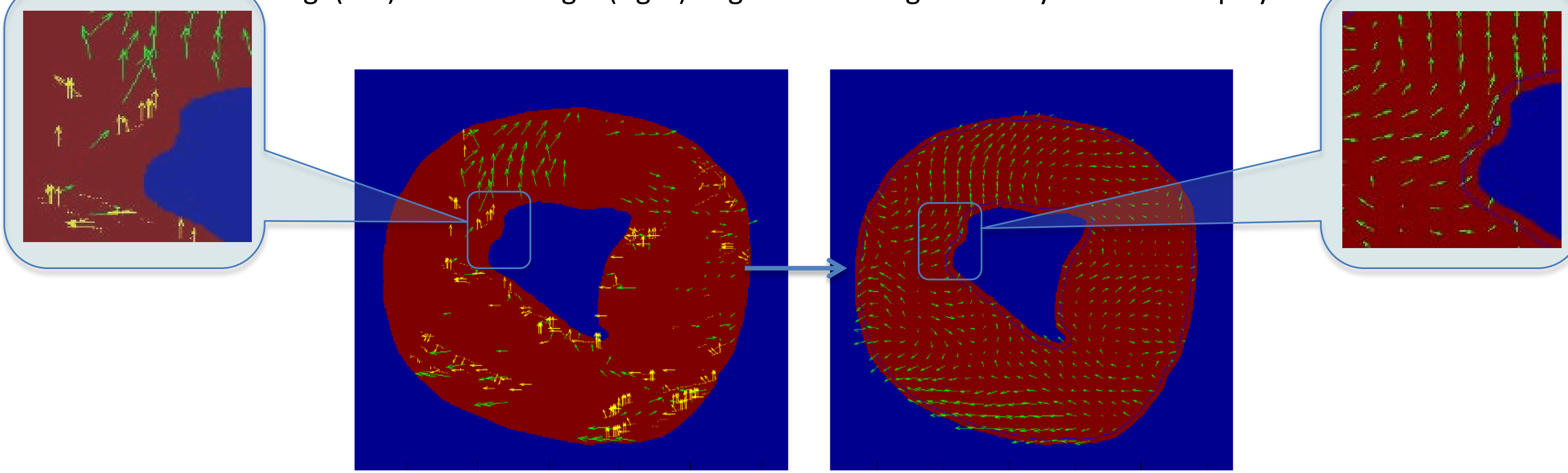

Fig: (Left) Sparse shape (yellow) and speckle (green) displacements. (Right) Dense displacement field.

Biomechanical information

- We are also looking to explore how we can possibly include biomechanical constraints into our estimation scheme that models how the myocardium deforms in reality.

- One such method is including the divergence free constraint to the displacement field. This is supposed to model the incompressibility property of the myocardium.

- We are looking into either using the divergence free RBFs (Lowitzsch 2002) or implicitly including the constraint into our objective function while minimizing it.

Towards 4D Stress Echocardiography

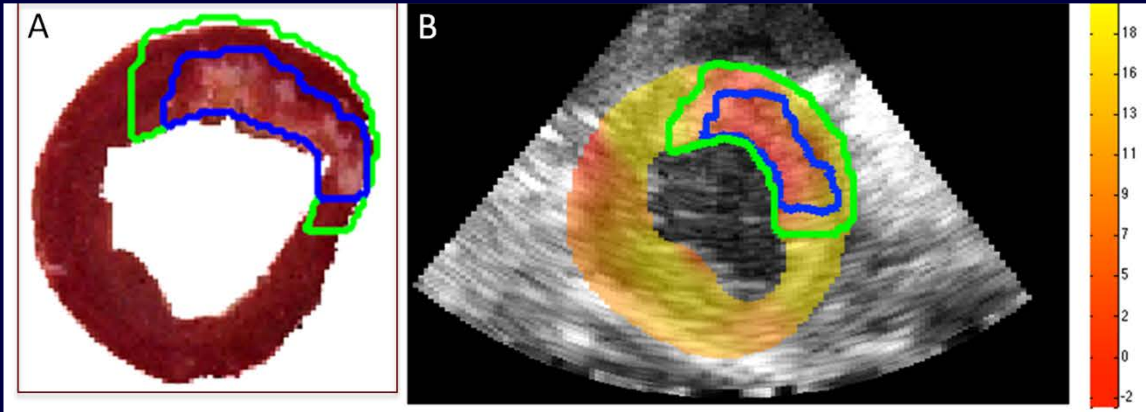

C	Mean ± Stdev Radial Strain %
Remote	18.3±6.7
Peri-infarct	10.9±7.3 p<.001 vs. rem
Infarct	6.0±6.7 p<.001 vs. peri

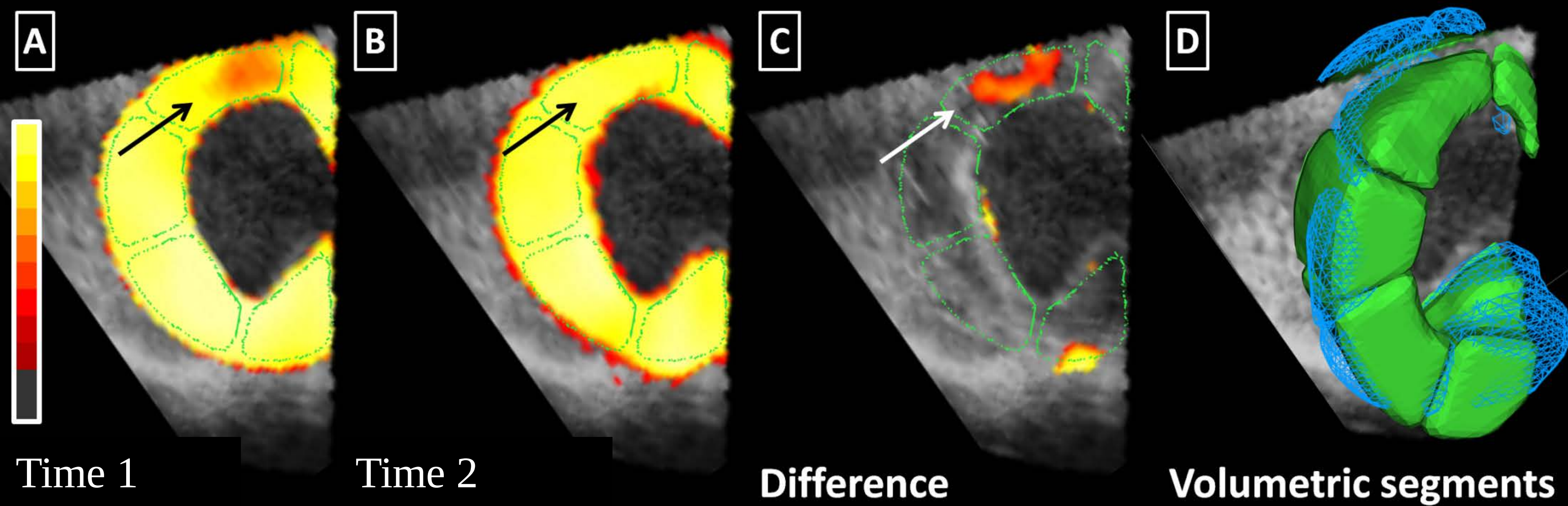

IV. Remaining Challenges

- Need to consider/model abnormal structure (e.g. infarcted regions---some of this happening w/ sparse coding)

- Move toward more complete temporal motion models.

- Consider formulating core algorithmic principles (e.g. statistical shape theory; sparsity)

- Develop robust validation/evaluation strategies including development of common (training and testing) databases

Colleagues/Collaborators

- *Segmentation* :

  -Larry Staib
  -Xiaolan Zeng
  -Hemant Tagare
  -Jing Yang
  - Xiaojie Huang

- *Cardiac Deformation*:

  - Xenios Papademetris
  - Colin Compas
  -Albert Sinusas, M.D.
  - Xiaojie Huang
  - Ping Yan
  - Yun Zhu
  -Smita Sampath
  - Nripesh Parajuli
  - Matt O'Donnell

Acknowledgements/ Software

- This work funded by NIH grants:

  R01HL082640 (BRP- NHLBI)

  R01 HL121226 (NHLBI)

- Check out Bioimage Suite (www.bioimagesuite.org):

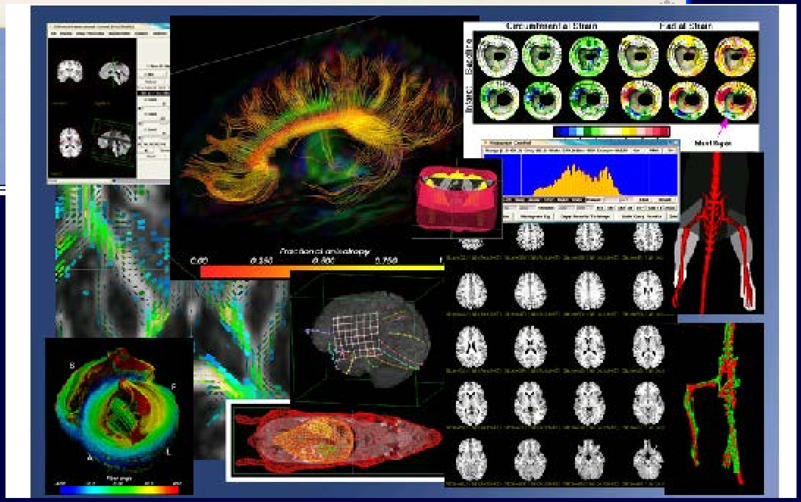

(developer: X. Papademetris)